Journal of Earth Science, *Vol. XX*, *No. XX*, *p. 1–13*, *Online 2022* *ISSN 1674-487X*
Printed in China
https://doi.org/10.1007/s12583-021-1579-8

Compositional Features of Fine Sediments Involved in the Montescaglioso Landslide (Southern Italy)

Vito Summa[1], **Rosa Sinisi**[*1], **Eleonora Paris**[2], **Agnese Emanuela Bonomo**[1]
1. *National Research Council*, *Institute of Methodologies for Environmental Analysis*, *C/da S. Loja* 85050, *Tito Scalo*, *Italy*
2. *School of Science and Technology*, *Geology Division*, *University of Camerino*, 62032 *Camerino*, *Italy*
Vito Summa: https://orcid.org/0000-0002-1345-5683; Rosa Sinisi: https://orcid.org/0000-0003-4439-3419

ABSTRACT: This paper presents the multidisciplinary study of the southern Italy Plio-Pleistocene sediments involved in the large Montescaglioso Landslide. The principal aim of the work is to assess the compositional characters (i.e., grain-size, mineralogy, petrography and geochemistry) and some rheological features (Atterberg's limits, plasticity index and activity) of these sediments to enrich our knowledge about the Montescaglioso fine sediments and correlation among the lithological properties studied. Two types of sediments, from a deep geognostic borehole and from the surrounding landslide area, were collected and analysed. No significant compositional differences have been found between the core and landslide area sediments. Conversely, some changes have been detected in sediments along the core. Particularly, the -15 to -20 m lithostratigraphic level hosts the highest percentages of phyllosilicates and clay fraction (CF), commonly considered as possible hazard factors for the landslide triggering. Further more, in the studied core sediments, the CF contents correlate with the Atterberg's liquid and plastic limits and a CF value of about 38% was suggested as threshold value for the changing of index properties of sediments. Other factors, such as the weathering degree and clay mineral type, do not show significant correlations with the rheological properties of sediments here studied.
KEY WORDS: grain-size, mineralogy, geochemistry, index properties, Plio-Pleistocene, sediments.

0 INTRODUCTION

Landslide phenomena involve different types of rocks, sediments and terrains anywhere in the world. The mass movements are determined by the action, often concomitant, of triggering factors such as temperature and climate changes, variation of precipitation regime, earthquake shaking, volcanism and human activities (Gariano and Guzzetti, 2016; Dai et al., 2002). Besides the triggering factor, inherent properties of slopes (including hydrogeochemical and geomorphological conditions) and terrains (as lithological, compositional and geotechnical features) play a key role in the slope instability and landscape evolution. In particular, as regards lithology, it was demonstrated that mineralogy of terrains involved into a mass movement may represent an important issue for the understanding of sliding events. Several authors (Mesri and Cepeda-Diaz, 1986;Kenney, 1977, 1967; Skempton, 1964) stated that clay minerals type and amount influence the rheology of fine sediments, i.e., terrains with a predominant clayey and silty component. Recently, Summa et al. (2018, 2015, 2010) demonstrated that in some landslides of southern Italy, affecting Plio-Pleistocene sedimentary sequences, kaolinite is in close relation with the geotechnical parameters of sediments (c, coesion; and φ, friction angle) and that this clay mineral often concentrates at the sliding surface of landslide body. In correspondence of the slip zone, high values of weathering indices also occur, suggesting weathering and alteration degree have a certain influence on stability of a sediment (Summa et al., 2018).

In southern Apennine (southern Italy), a number of rainfall-induced landslides widely occur, mainly affecting the exposed sedimentary sequences (Giannecchini et al., 2016; Napolitano et al., 2016; Rosi et al., 2012; Guzzetti and Tonelli, 2004; Guzzetti et al., 1994). The Montescaglioso Landslide (Basilicata Region, Italy) is one of these and represents a large mass movement that involved the southern slope of a hill consisting of a part of the Plio-Pleistocene sedimentary sequence of the Bradanic Trough. Several studies have been focused on this event so far, providing a comprehensive description of the phenomenon mostly in terms of geomorphological features (Amanti et al., 2016; Pellicani et al., 2016; Manconi et al., 2014) and landslide displacements, mechanism and movement directions (Pellicani et al., 2019; Caporossi et al., 2018; Bozzano et al., 2017; Raspini et al., 2015). However, these studies, mainly devoted to geological surveys and remote sensing mapping and monitoring techniques, completely neglected the role of compositional characters of landslide terrains.

With this in mind, this work, which represents the first step of a more comprehensive study, is aimed to fill the knowl-

*Corresponding author: rosa.sinisi@imaa.cnr.it

Manuscript received August 26, 2021.
Manuscript accepted November 22, 2021.

Summa Vito, Sinisi Rosa, Paris Eleonora, Bonomo Agnese Emanuela, 2022. Compositional Features of Fine Sediments Involved in the Montescaglioso Landslide (Southern Italy). *Journal of Earth Science*, XX(XX): 1–13. https://doi.org/10.1007/s12583-021-1579-8. http://en.earth-science.net

edge gap on lithological aspects of sediments involved in the Montescaglioso Landslide. A detailed study of the compositional characteristics (as granulometry, bulk and clay fraction mineralogy, petrography and geochemistry) and some index properties (Atterberg's limits, plasticity index and activity) of the landslide sediments are here proposed along with the preliminary correlations between composition and rheological properties of the studied sediments. According to previous authors (Summa et al., 2018, 2015, 2010, 2007), this study suggests that a multidisciplinary approach is needed for studying landslides in fine sediments all-over in the world, in order to effectively contribute to the assessment of hazard conditions inducing the mass movements.

1 GEOLOGICAL, STRATIGRAPHICAL AND GEOMORPHOLOGICAL SETTING OF THE AREA

The study area is close to the Montescaglioso Village (Fig. 1a), a little town of southern Italy (Matera Province, Basilicata Region), located at a hill top (about 400 m a.s.l.) in the Bradanic Trough. The latter represents the foredeep of the southern Apennines, lying between the Apulian foreland to the east and the Apennine chain to the west. Plio-Pleistocene marine and continental sediments infill the Bardanic Trough, forming a coarsening upward, regression sequence (Tropeano et al., 2002). In the study area, most of such depositional sequence is largely exposed. In detail, from the top downward the outcropping sediments consist mainly of clays and silty clays of the Argille Subappennine Formation (Middle to Late Pliocene) and subordinately of sands, belonging to the Monte Marano Formation (Late Pliocene), and calcarenites of the Monte Castiglione Formation (Late Pliocene–Calabrian) (Fig. 1a). Polygenic gravels and sandy conglomerates of terraced deposits complete the Plio-Pleistocene sedimentary sequence.

In Fig. 2, a schema of stratigraphy and sampling along the S3 borehole is shown. According to Bonomo (2015), the core sediments are made up of four main lithological levels that, from the top to the bottom of survey, consist of: (1) a detrital cover (0 to -3.9 m) that includes a 1 m-thick anthropic debris and loose detrital landslide and slope terrains made up of heterometric, rounded and sub-rounded carbonate and siliceous clasts embedded in a sandy carbonate matrix; (2) brown and brownish sandy gravel (-3.8 to -5.9 m) having carbonate as much as siliceous clastic elements with variable millimetre to centimetre size. Between -4.8 and -5.0 m, a yellow-greenish, more plastic level, also rich in carbonate microfossils, was detected and sampled (S3C1 sample); (3) a thick level of yellowish silty clays and clayey silts (-5.9 to -12.5 m). At the top of this level (between -5.9 and -6.4 m), it is possible to distinguish a sandy-gravelly layer (S3C3 sample), with clasts very similar to those of the overlying brownish gravelly level. In addition, frequent wet soil layers with black and/or brown nodules and yellowish pervasive oxidation bands (i.e., salbands sensu Brondi et al., 1993) were observed at different stratigraphic positions. In particular, the oxidized bands were sampled between -8.0 and -8.5 m (S3C6 sample), -10.0 and -10.7 m (S3C8 sample), -11.5 and -12 m (S3C10 sample); (4) a thick level of bluish-grey, medium- to fine-grained silt from compacted to strongly compacted (-12.5 to -25 m). In the upper portion, this level is characterized by a yellowish to greyish transition zone (between -12.5 and -14 m; S3C11 and S3C12 samples) that definitely ends with a thin silty layer including reddish nodules (from -14.7 to -15 m; S3C14 sample). Starting from this depth down to about -20 m, samples show low plasticity and an increased ability to rupture along plain-parallel surfaces. Downward (from -20.5 to -25 m), the bluish-grey silts are strongly compacted and display a major content of the sandy component at place represented also by fossil remnants (-20.6 to -20.9 m; S3C20 and S3C21 samples).

In the surroundings of the Montescaglioso Hill, numerous examples of land degradation phenomena (such as erosion gullies, linear type erosion, flow landslide, creep, rotational slips, collapses) occur, playing a significant role in the morphological evolution of the hill slopes. The presence of several depositional sequences, heterogeneous sediments and interconnected morphotypes, resulting from the complex sedimentary and climatic history of the area during the Pleistocene, contribute to the slope instability.

The studied landslide is located SW of the Montescaglioso urban area and represents the reactivated portion of a wider and deeper landslide that affected the area in the past (Figs. 1a and 1b) (Carlà et al., 2016; D'Ecclesiis and Lorenzo, 2006). The landslide is about 1.2 km in length and 800 m in width, involving a total area of about 300 km^2 (Manconi et al., 2014). As documented by several authors, the movement occurred after 56 hours of continuous and intense rainfalls (>70% of the mean annual precipitation; Manconi et al., 2014) that seem to be the principal cause of the landslide triggering. From a geomorphological point of view, recent studies revealed that the landslide slope was affected by severe morphological changes including a general 5–6 m lowering of the ground quote at the detachment zone, and a 6–8 m increasing (up to a maximum of 13 m) in the accumulation zone. The prevailing slipping mechanism was translational with a 5° rotational component.

2 SAMPLING AND ANALYTICAL METHODS

This study presents and analyses data regarding the compositional features, the granulometry and some index properties of numerous samples representative of the sediments involved in the Montescaglioso Landslide. In detail, 13 samples (hereafter "widespread sediments/samples") are sediments randomly distributed in the landslide area, of which eight samples are deep sediments (S1, S2C1, S2C2, S2C3, S4, S5, S6, S7) collected at depths between -3.5 and -65 m (Table 1) from deep boreholes carried out in the landslide area, and four are shallow sediments (MS2, MS3, MS4, MS6) collected along the exposed surface of the outcrops (Fig. 1b); twenty-four samples (from S3C1 to S3C24, hereafter "core sediments/samples") are sediments of the S3 deep borehole, sampled at different stratigraphical positions along the core (Fig. 1b). Such a borehole is a 25 meters-long geognostic survey that was performed on March 2014 by continuous rotating core drilling, $\varnothing$ = 101 mm, and represents to date an opportunity for studying the stratigraphical and compositional features of the sediments composing the Argille Subappennine Formation.

The widespread sediments as much as the S3 core sediments were subjected to the grain-size and X-ray diffraction

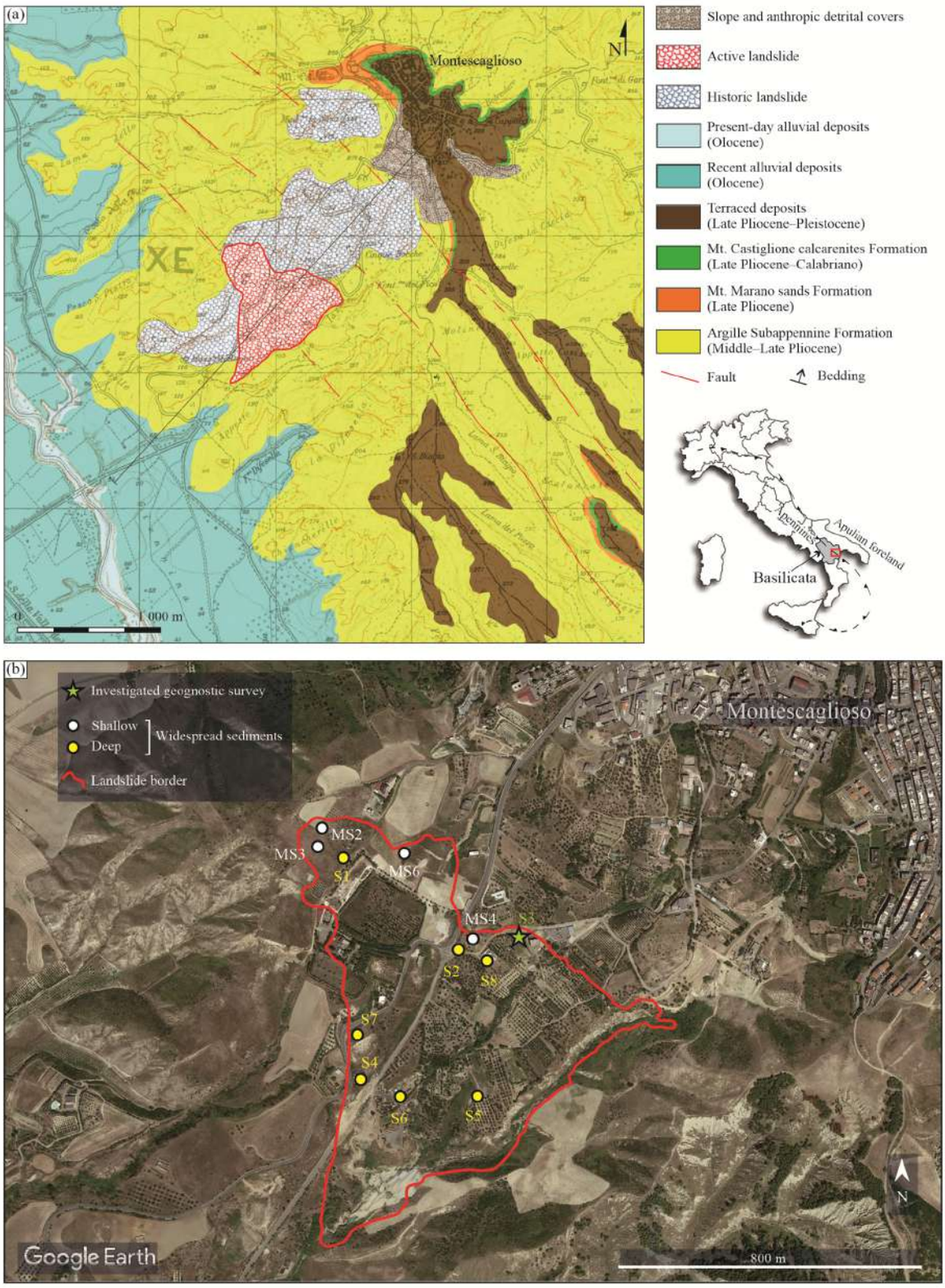

Figure 1. (a) Geological map of the investigated area (modified after Bonomo, 2015). (b) Location of sampling sites of the widespread sediments and S3 borehole. The landslide border is from Perrone et al. (2014).

(XRD) analyses at the Laboratorio di Geologia Medica e Ambientale of the Institute of Methodologies for Environmental Analysis of the National Research Council of Italy (CNR-IMAA). The grain-size analysis has been carried out using the wet sieving, to separate granulometric fractions between 2 mm and 63 μm, and fractioned sedimentation methods, to obtain the fractions ranging from 63 to <2 μm, following the Stokes' Law as described by Summa (2000). The qualitative and quan-

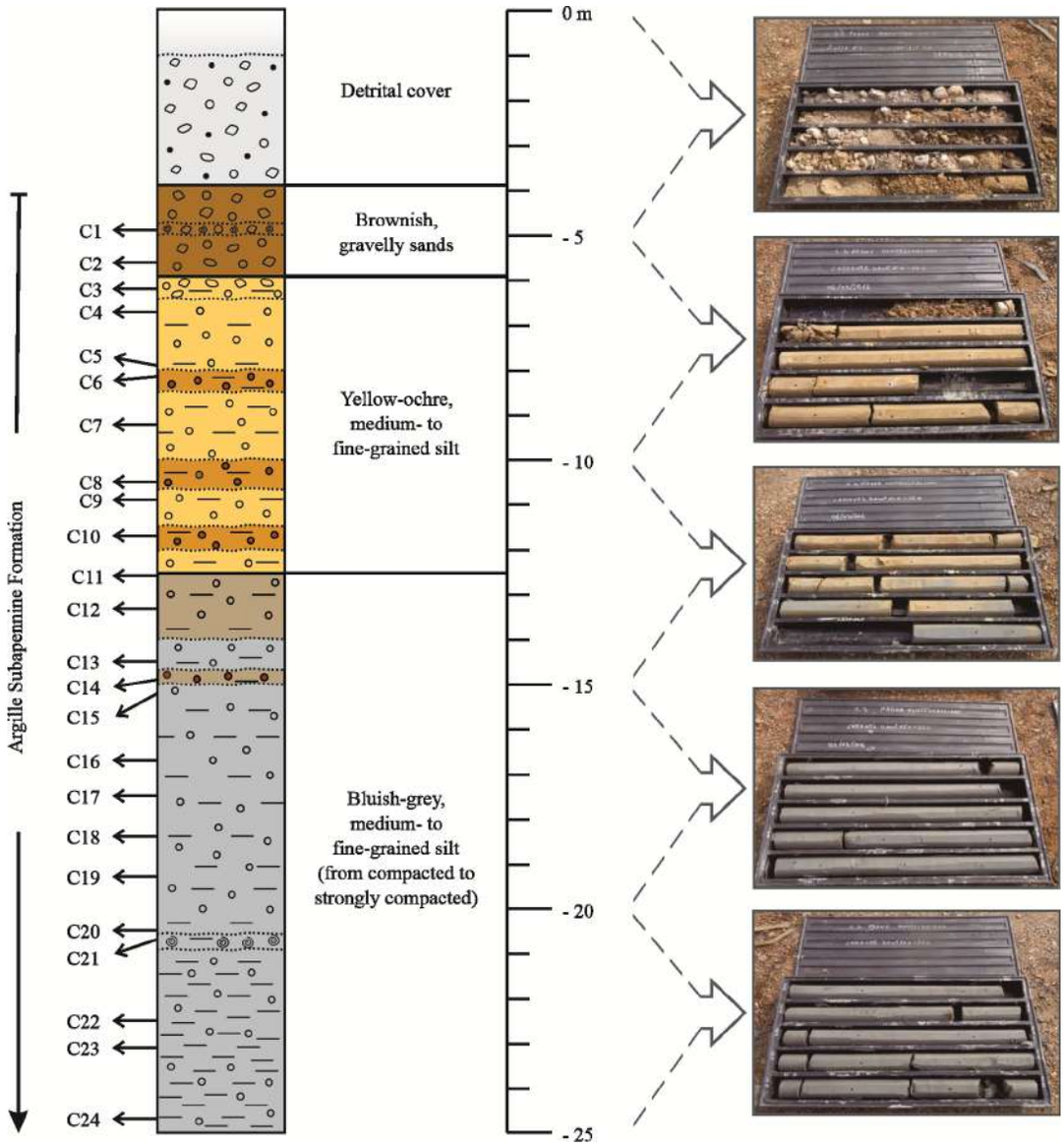

Figure 2. Stratigraphic sequence of the S3 survey and position of the investigated samples along the sediment core.

titative mineralogical analyses by XRD have been performed on powdered sediments using a Rigaku D/MAX-2200/PC diffractometer with a "theta-theta" configuration and a curved graphite crystal monochromator (Cu kα, 40 kW, 30 mA, 3 sec/step, 0.02° 2θ). Random specimens were used for the mineral identification of bulk samples; oriented specimens were used for the analyses of the clay fraction (CF, <2 μm). Prior to the analysis, the oriented samples were subjected to chemical treatments, including magnesium chloride saturation and glycolization (8 hours at 60 °C), and heating at 375 °C in a muffle furnace (Cavalcante et al., 2007; Schultz, 1964). The quantitative determination of minerals in the bulk samples and in the <2 μm fractions has been performed according to Cavalcante et al. (2007), Shaw et al. (1971), Schultz (1964), using the X'Pert HighScore Plus v.2.1.b (PANalytical B.V. 2005) software.

Both types of samples (widespread and S3 core) have been analysed also for the determination of liquid limit (w_L), plastic limit (w_P) and plasticity index (PI) that were accomplished in accordance with the ASTM (2007) method and recommendations.

In addition, due to the great importance of S3 core sediments for this study, further analyses were reserved to these samples. In particular, the X-ray fluorescence spectrometry (XRF) was used to chemically characterize the S3 samples in terms of wt.% of major element oxides (including Si, Al, Fe, Ca, Na, Mg, K, Mn, Ti, and P). Elemental analyses were obtained on pressed powder disks of bulk sediments at the XRF Laboratory of the Dip. Scienze della Terra e Geoambientali, University of Bari (Italy). A PANalytical Axios advanced spectrometer with Rh SST-mAX radiation was used and the matrix effect was corrected following the methods of Franzini et al. (1975, 1972). Loss on ignition (LOI) was determined after heating samples overnight at 900 °C.

3 RESULTS

3.1 Granulometry

From a granulometric point of view, no significant difference between widespread and S3 core sediments has been ob-

Table 1 Results of the grain-size analysis and granulometrical classification of the studied sediments

Sample	Depth (m)	Grain-size fractions (%)												Classification by Blott and Pye (2012)
		>2 mm	2–1 mm	1–0.5 mm	0.5–0.25 mm	250–125 µm	125–63 µm	63–32 µm	32–16 µm	16–8 µm	8–4 µm	4–2 µm	<2 µm	
		Gravel	VC sa	C sa	M sa	F sa	VF sa	VC si	C si	M si	F si	VF si	Clay	
Widespread samples														
S1	8.5	-	-	-	-	1	9	16	14	16	12	17	15	Slightly sandy, slightly clayey silt
S2C1	3.5	-	-	-	-	-	2	14	17	17	15	9	26	Very slightly sandy, clayey silt
S2C2	10	-	-	-	-	1	6	18	14	13	14	13	20	Slightly sandy, clayey silt
S2C3	21	-	-	-	-	1	15	19	12	9	8	12	23	Slightly sandy, clayey silt
S4	8.5	-	-	-	-	-	3	17	18	17	11	11	23	Very slightly sandy, clayey silt
S5	10	-	-	-	-	1	5	12	13	18	16	12	23	Very slightly sandy, clayey silt
S6	65	2	-	-	-	9	30	13	10	8	8	6	12	Sandy clayey silt
S7	7	-	-	-	-	-	4	14	16	15	15	7	30	Very slightly sandy, clayey silt
MS2	0.74	1	-	-	-	1	4	9	9	13	16	15	32	Slightly sandy, clayey silt
MS3	0.45	1	-	-	1	1	3	10	12	13	18	12	27	Slightly sandy, clayey silt
MS4	6	-	-	-	-	-	4	20	17	16	13	9	20	Slightly sandy, clayey silt
MS6	1.8	-	-	-	-	-	7	14	19	16	14	9	21	Slightly sandy, clayey silt
S3 core sediments														
S3C1	4.9	4	2	2	3	15	8	7	7	11	13	12	15	Slightly clayey, sandy silt
S3C2	5.6	3	2	3	15	45	9	5	3	3	3	5	4	Slightly clayey, silty sand
S3C3	6.2	9	-	-	-	-	2	15	15	16	13	12	17	Very slightly sandy, slightly clayey silt
S3C4	6.7	-	-	-	-	1	6	22	18	16	11	10	14	Slightly sandy, slightly clayey silt
S3C5	7.9	-	-	-	-	1	6	20	19	17	13	6	17	Slightly sandy, slightly clayey silt
S3C6	8	-	-	-	-	-	3	15	19	19	13	11	19	Very slightly sandy, slightly clayey silt
S3C7	9.2	-	-	-	-	1	6	22	14	16	12	11	18	Slightly sandy, slightly clayey silt
S3C8	10.5	-	-	-	-	-	2	13	17	17	16	10	25	Very slightly sandy, clayey silt
S3C9	10.9	-	-	-	-	-	1	11	15	16	18	15	24	Very slightly sandy, clayey silt
S3C10	11.7	-	-	-	-	2	11	19	16	14	10	7	21	Slightly sandy, clayey silt
S3C11	12.6	-	-	-	-	-	4	15	15	17	14	13	22	Slightly sandy, clayey silt
S3C12	13.3	-	-	-	-	1	15	21	16	13	11	8	16	Slightly sandy, slightly clayey silt
S3C13	14.5	-	-	-	-	-	4	14	14	15	11	14	28	Slightly sandy, clayey silt
S3C14	14.9	-	-	-	-	-	3	15	15	14	11	18	24	Very slightly sandy, clayey silt
S3C15	15.2	-	-	-	-	-	2	7	8	10	14	11	47	Very slightly sandy, clayey silt
S3C16	16.7	-	-	-	-	-	2	11	11	13	13	10	40	Very slightly sandy, clayey silt
S3C17	17.5	-	-	-	-	-	3	9	10	12	15	10	41	Very slightly sandy, clayey silt
S3C18	18.4	-	-	-	-	-	1	6	8	10	13	12	49	Clayey Silt
S3C19	19.3	-	-	-	-	-	1	7	7	11	15	12	48	Clayey Silt
S3C20	20.5	1	-	-	1	4	14	14	8	7	8	10	32	Sandy clayey silt
S3C21	20.7	-	-	-	-	3	25	11	9	8	8	8	28	Sandy clayey silt
S3C22	22.5	-	-	-	-	3	19	21	9	9	8	5	26	Sandy clayey silt
S3C23	23.1	-	-	-	-	1	15	21	11	10	8	6	28	Slightly sandy, clayey silt
S3C24	24.7	-	-	-	-	2	21	15	8	12	8	7	27	Sandy clayey silt

VC. Very coarse; C. coarse; M. medium; F. fine; VF. very fine; sa. sand; si. silt.

served on the basis of their percentages of sand (>63 µm to <2 mm), silt (>2 to <63 µm) and clay (<2 µm). All investigated samples, due to their >50% silt component, mainly fall in the field of silty sediments with the only exception represented by the S3C2 sample. This sample having high amount of the sandy component (75%) and low silt and clay percentages (21% and 4% respectively) stays within the sandy sediments field.

Details of all grain-size fractions detected in the widespread and S3 core sediments are reported in Table 1 where the sediment classification by Blott and Pye (2012) is also shown. Comparing the two sample groups, a strong granulometrical similarity between them is evident, confirming the above observa-

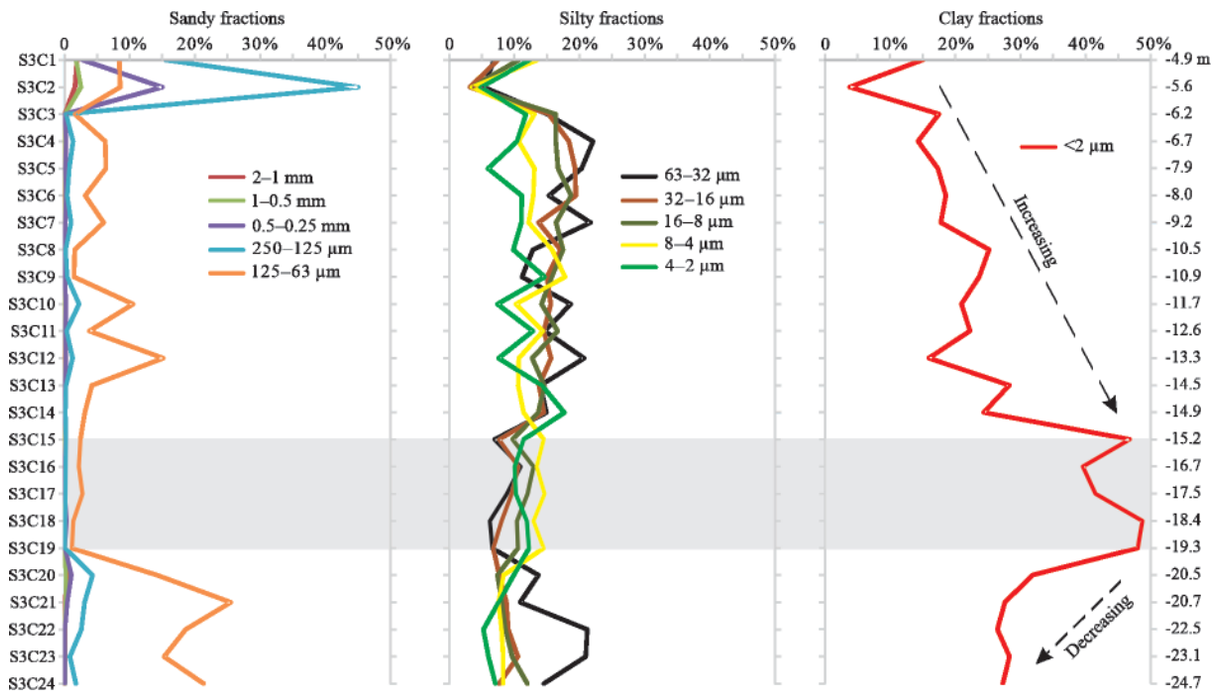

Figure 3. Distribution of granulometric fractions (sandy, silty and clayey) along the S3 survey.

tions and suggesting the sediment homogeneity in the study area.

As for the S3 core sediments only, the distribution of detailed grain-size fractions along the profile (Fig. 3) has revealed that silty fractions are the main granulometrical components of sediments throughout the core, starting from -6 m (S3C3 sample) downward. Although such fractions have narrow variation ranges, in general the coarser (mainly 63–32 and 32–16 µm) and the finer (32–16 to 4–20 µm) ones show opposite trends. This is also the case of the distribution of sandy and clay fractions. In particular, among the sand, the 125–63 µm fraction oppositely varies with the <2 µm content. The latter, despite the fluctuations along the profile, shows an increasing trend up to -15 m of depth (S3C15 sample) and a decreasing trend from -20 m (S3C19 sample) downward. As a consequence, sediments with the highest amounts of clay (40% to 49%) occur in the stratigraphical interval between -15 and -20 m, which corresponds to the compacted to strongly compacted transition zone of the bluish-grey silt (see Fig. 2).

3.2 Mineralogy and Petrography

The mineralogical composition of the investigated sediments is summarized in Table 2 where XRD data on bulk and <2 µm specimens of both widespread and S3 core samples are shown. Comparing the two sediment groups, no significant compositional difference was found.

All widespread samples result as carbonate-rich siliciclastic sediments that consist of phyllosilicates, as principal mineralogical phase (mean value = 60%), and carbonates (calcite and dolomite, mean values = 17% and 4% respectively), quartz (mean value = 12%), plagioclase (mean value = 5%) and K-feldspar (mean value = 2%) as subordinate minerals. The XRD analyses of the <2 µm fractions revealed that in these samples a high percentage of the interlayered I/S clay mineral is present varying in the 66%–80% range. Other TO and TOT minerals, as kaolinite (7% to 11%), chlorite (3% to 6%) and illite-muscovite (8% to 11%) are in all investigated samples with contents lower than the interlayered I/S ones.

Similar to the other sediments of the landslide area, the mineralogical composition of bulk samples of the S3 core mainly includes phyllosilicates, calcite, quartz, plagioclase, dolomite and K-feldspar as principal mineral phases (Table 2). Phyllosilicates are the most abundant mineralogical component, showing ΣPhyl values higher than 50% in all samples except for the shallow S3C2 sample that has total phyllosilicates equal to 28%. Such a sample, conversely, is the richest in quartz (31%). The remaining core samples show comparable quartz contents ranging from 3% to 9%. Among the carbonate minerals detected (calcite and dolomite), calcite is the prevailing phase in all samples, reaching its highest contents (21%) in the shallow S3C1 and S3C2 samples. These samples are also rich in plagioclase and K-feldspar compared with the other core samples, with abundances of Pl = 6% and 10%, and Kls = 3% and 10% respectively.

The phyllosilicate minerals detected in the <2 µm fraction of core sediments are represented by the interlayered I/S, illite-mica, kaolinite and chlorite (Table 2). Again, interlayered minerals represent most of the total phyllosilicates present, with percentages ranging between 61% and 87%. Illite-mica, kaolinite and chlorite are in subordinate amounts being between 4% and 23%, 4% and 13%, trace and 10%, respectively. Observing the distribution of phyllosilicate components with the depth, a decreasing trend of the interlayered clays abundances and a slight increasing trend of the other phyllosilicate minerals was detected. Regardless of trend, it is of note that a significant variation of I/S amounts affects the S3C16 (I/S = 57%) to S3C18 (I/S = 75%) samples that fall into the stratigraphic level with the highest content of clay fraction.

Petrographical observations were also performed on some

Table 2 Results of the quantitative XRD analysis of bulk and <2 μm specimens of the studied sediments

Sample	Depth (m)	Bulk (%)						<2 μm (%)			
		Qtz	Cal	Dol	Kfs	Pl	ΣPhyl	Kln	Chl	Ilt-Ms	I/S
Widespread sediments											
S1	8.5	11	12	tr	6	10	58	8	6	10	66
S2C1	3.5	14	15	7	tr	7	56	10	tr	8	79
S2C2	10	12	18	7	tr	4	58	7	5	8	80
S2C3	21	13	18	4	tr	6	58	8	5	10	77
S4	8.5	12	16	tr	tr	tr	65	11	tr	11	75
S5	10	12	16	tr	tr	tr	66	10	5	8	77
S6	65	18	23	6	5	9	39	8	6	9	77
S7	7	10	12	5	tr	tr	69	11	5	11	73
MS2	0.74	8	20	tr	tr	4	66	9	tr	9	79
MS3	0.45	10	19	tr	tr	4	64	10	5	11	74
MS4	6	12	23	7	tr	5	50	8	tr	9	80
MS6	1.8	11	16	5	tr	tr	64	11	4	11	74
S3 core sediments											
S3C1	4.9	9	21	-	6	tr	62	7	tr	4	87
S3C2	5.6	31	21	tr	10	10	28	4	tr	7	87
S3C3	6.2	8	16	tr	tr	5	67	6	tr	7	85
S3C4	6.7	7	11	4	tr	4	72	6	tr	9	83
S3C5	7.9	8	12	tr	tr	4	73	7	tr	7	84
S3C6	8	6	7	tr	tr	tr	82	6	tr	8	83
S3C7	9.2	4	6	tr	tr	tr	87	5	tr	9	83
S3C8	10.5	4	6	tr	tr	tr	85	8	tr	10	80
S3C9	10.9	5	6	tr	tr	tr	84	6	tr	8	83
S3C10	11.7	6	10	tr	4	4	74	6	tr	10	81
S3C11	12.6	7	11	tr	tr	tr	75	7	tr	11	78
S3C12	13.3	6	10	8	tr	10	64	8	5	13	74
S3C13	14.5	5	9	tr	tr	tr	80	11	8	13	69
S3C14	14.9	6	9	tr	tr	tr	78	12	8	14	65
S3C15	15.2	5	9	tr	tr	tr	82	11	7	14	68
S3C16	16.7	5	8	tr	tr	tr	84	11	9	23	57
S3C17	17.5	tr	6	tr	tr	tr	88	10	7	11	72
S3C18	18.4	tr	7	tr	tr	tr	87	9	6	10	75
S3C19	19.3	4	7	tr	tr	tr	84	13	8	14	65
S3C20	20.5	4	8	tr	tr	4	80	11	8	13	67
S3C21	20.7	8	9	tr	tr	tr	75	10	8	17	65
S3C22	22.5	6	6	tr	tr	tr	80	10	9	14	67
S3C23	23.1	5	8	tr	tr	5	76	11	9	21	59
S3C24	24.7	8	8	4	4	10	66	11	10	18	61

Qtz. Quartz; Cal. calcite; Dol. dolomite; Kfs. K-feldspar; Pl. plagioclase; ΣPhyl. total phyllosilicates; Kln. kaolinite; Chl. chlorite; Ilt. illite; Ms. muscovite; I/S. interlayered illite/smectite. tr is for trace (0–3%); - is for "not detected". Minerals' abbreviations are as suggested by Whitney and Evans (2010).

core samples selected by macroscopic characters as the colour of sediments and the presence of millimetre pervasive fracturing associated to yellowish and yellow-ochre salbands. Any significant variation of texture wasn't detected. In general, samples of the yellowish and blue-greyish silts differ by the relative amount of opaque iron-bearing phases (oxides and hydroxides) in the matrix. A major presence of such oxides characterize the yellowish sediments. In all samples, it was observed a skeleton consisting of millimetre (yellowish silts) to nanometre (blue-greyish silts) silicate clasts, mainly quartz and feldspars, that are embedded in a clayey carbonate matrix. However in the yellowish sediments, the millimetre clasts prevail on the nanometre ones. Where veining and fracturing are present, calcite and/or iron oxides and hydroxides infill the

veins and fractures, suggesting their secondary formation during a post-diagenetic phase. Remnants of microfossils as foraminifera, bivalves and gastropods are common in the studied sediments and concentrate mainly in the coarser samples where a poor sorting is also observed.

3.3 Chemical Composition

The chemical composition of the S3 core samples can be mainly described by four elements, Si, Al, Fe, and Ca. In fact, SiO_2 is the most abundant oxide ranging between 42.1 wt.% and 46.7 wt.%, with the exception of the S3C2 sample where it is much higher (68.2 wt.%). The CaO contents range between 12.1 wt.% and 21.2 wt.% with the S3C1 sample having the highest value of the whole set of core samples. The Al_2O_3 and Fe_2O_3 respectively vary in the ranges of 5.3 wt.%–13.5 wt.% and 2.3 wt.%–6.0 wt.% and both show the lowest contents in the S3C2 sample. Among the other major element oxides, MgO and K_2O are characterized by narrow ranges of percentage variation and very similar average values of 2.4 wt.% and 2.0 wt.% respectively. The Na_2O, MnO, TiO and P_2O_5 have the lowest amounts that rarely exceed 1.0 wt.%.

As to the distribution of major elements with depth (Fig. 4), the most relevant observation regards the opposite trend of Al_2O_3 and CaO contents along the sediment core with the exception of the S3C1 and S3C2 samples, which again differs from the other samples. The Al_2O_3 and CaO trends suggest that these oxides are independent from each other and consequently the CaO contents account for the carbonate minerals only.

3.4 Rheological Parameters: Atterberg's Limits, Plasticity Index, Activity

The Atterberg's limits (liquid limit, w_L; plastic limit, w_P), the plasticity index (PI= w_L–w_P) and activity (Ia = PI/CF where CF is the clay fraction) of the studied widespread and S3 core sediments were detected.

In the widespread sediments, w_P varies between 16% (S6) and 23.5% (MS3) with a mean value of 20.9%; the w_L values are in the 33.8% (S6) – 65% (MS2) range having a mean of 52.9%; the PI and Ia are respectively from 17.8% (S6) to 43.3% (MS2) (mean value = 31.9%) and from 1% (S7) to 2.3% (S1) (mean value = 1.4%).

In the S3 core sediments, the w_P values vary from 33% (S3C18) to 16% (S3C12) with a mean of 22%, whereas the w_L varies from 42% (S3C12) to 86% (S3C18) with a mean value of 58%. The sediments have a mean PI value equal to 36%, deriving from values ranging between 23% (S3C24) and 55% (S3C15). These data suggest that the core sediments are predominantly "plastic" except for some samples from the upper portion of the borehole (S3C2, S3C3, and S3C8) and all samples falling in the -15 to -20 m stratigraphic level. There, the PI value increases and sediments are classified as "very plastic". Relatively to the activity, it is worth noting that downward

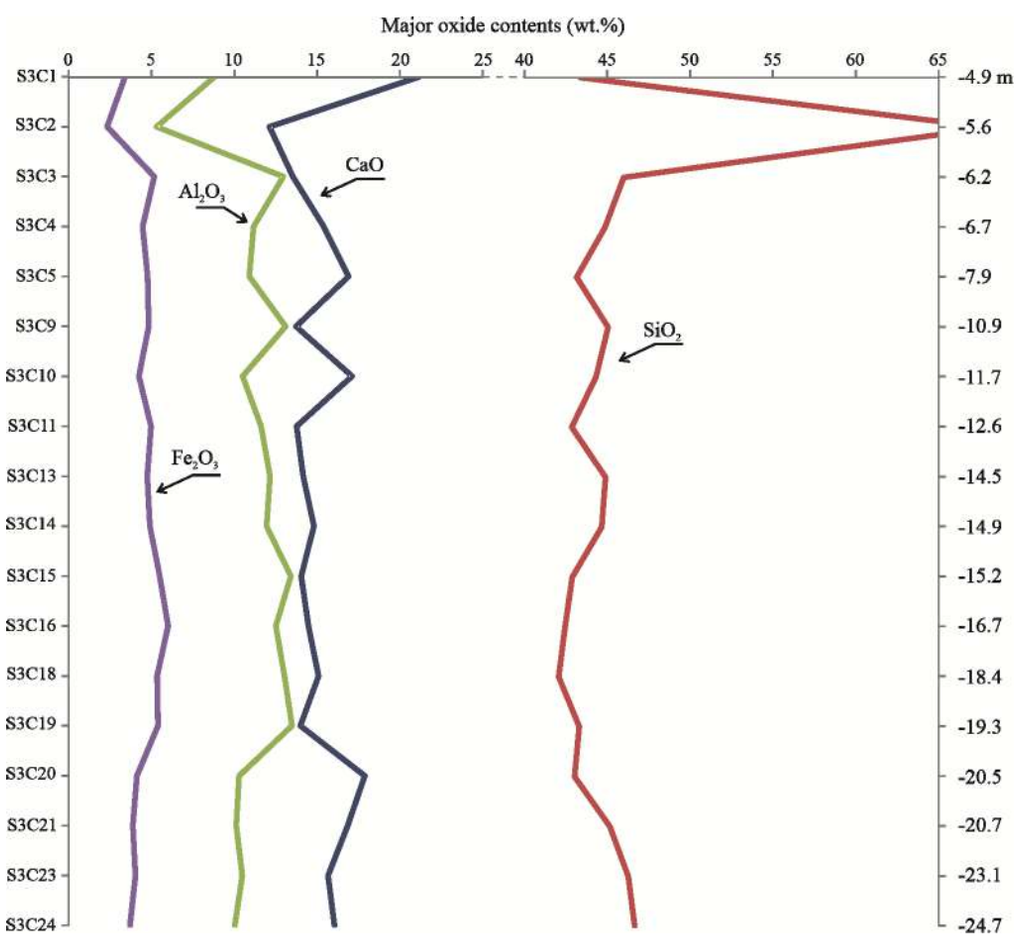

Figure 4. Variation of selected major elements (SiO_2, Al_2O_3, Fe_2O_3, and CaO) along the investigated S3 sediment core.

along the core a slight decreasing of the Ia parameter was detected, with a change from "active" to "normally active" status of sediments at about 15 m of depth.

4 DISCUSSION

As previously stated, the detailed study of the texture and composition of landslide terrains, aside from being useful for characterizing the sediments, may contribute to understanding the slope instability mechanisms.

According to the on field macroscopic observations, in the study area silts are mainly present, variously alternating to finer and/or coarser sediments. The alternation of granulometrically different levels was evidenced by the distribution of the grain size fractions along the investigated S3 core (Fig. 3) suggesting the presence of a heterogeneous sedimentary sequence. In particular, it is worthy of note that the presence of the stratigraphic level at depths between -15 and -20 m, where the samples characterized by the highest percentage of the <2 μm fraction (Fig. 3 and Table 1) and the highest phyllosilicates amounts (Table 2) are present.

It is well known that the quantity of clay fraction in a terrain can play a significant role in the triggering of a rainfall-induced landslide (Igwe, 2015; Igwe et al., 2014; Summa et al., 2010, 2007; Yalcin, 2007). In fact, generally, on comparable geomorphological, geological and climatic conditions, as the clay fraction content increases, the susceptibility of a slope to failure increases. The geochemical and granulometrical properties of clay minerals contribute to the reduction in the stability of a natural slope mostly when intense rainfalls occur causing both a rapid increasing of the soil water content and a worsening of the geotechnical properties of the material involved. In the study case also, the index properties of S3 core sediments seem to be influenced by the clay fraction content. In detail, as shown in Fig. 5, w_L and w_P values of S3 samples remain fairly constant up to 38% CF; above this value, w_L and w_P increase proportionally to CF. Although further investigations are needed, such variation paths could indicate the presence of a CF threshold value responsible for the changing of index properties of sediments.

As for widespread sediments, liquid and plastic limits do not show correlations with the clay fraction content. However, considering the geotechnical features of these samples recently published by Amanti et al. (2016) (Table 3), some relationships between granulometry and coesion (c) and friction angle (φ) seem to be significant. In particular, in our widespread sample set φ could be influenced by sediment granulometry and mostly by the 63–8 μm and 8–2 μm fractions that tend to correlate with it, respectively, positively and negatively (Fig. 6).

As already documented in other studies performed on Plio-Pleistocene fine sediments of Basilicata (Summa et al., 2018, 2010), also in the widespread samples of the Montescaglioso Landslide, c shows a negative correlation with the kaolinite content in the sediments (Fig. 7) supporting the idea that this mineral may affect the geotechnical behaviour of terrains.

As a consequence, regardless of the clay fraction amount, the type of clay minerals included in a landslide terrain may represent a key hazard factor in the possible activation of slip zones. Yalcin (2007), according to Ohlmacher (2000), suggested that terrains with illite and montmorillonite as principal clay minerals have higher swelling potentials and lower shear strengths than those composed of kaolinite and chlorite. Referring to the Montescaglioso Landslide sediments, we observe that the aforementioned S3 stratigraphic level (-15 to -20 m of depth), compared with the samples at shallower and deeper depths along the S3 core, is characterized by a higher content of kaolinite, a high content of chlorite and a lower amount of interlayered illite/smectite minerals in the <2 μm fraction. This

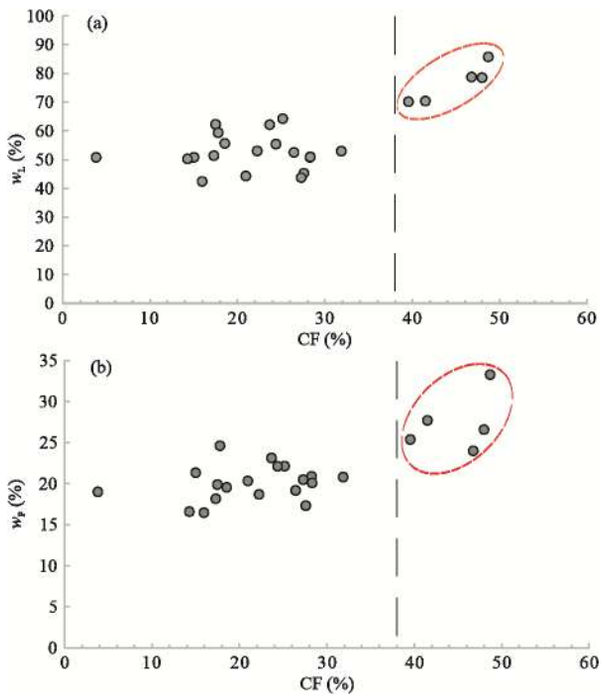

Figure 5. Variation of (a) liquid limit (w_L) and (b) plastic limit (w_P) with the clay fraction content (CF, <2 μm fraction) of studied S3 core sediments. Red circles display core samples from the -15 to -20 m level. See the text for further details.

Table 3 Geotechnical parameters of widespread samples collected in the Montescaglioso Landslide area

Test	Samples	Depth (m)	c' (kPa)	φ' (°)
Direct shear test	MS2	0.7	16	26
	MS3	0.5	20	20
	MS4	6.0	1	39
	MS6	1.8	1	41
	S5	53.0	53	23
	S6	41.5	42	19
	S2	10.0	47	24
	S1	8.5	28	24
	S2	3.5	23	33
	S4	8.5	34	29
	S7	10.5	21	30
	S3	8.0	21	26
	S7	3.0	20	36

Data, referring to results of the direct shear test, are from Amanti et al. (2016).

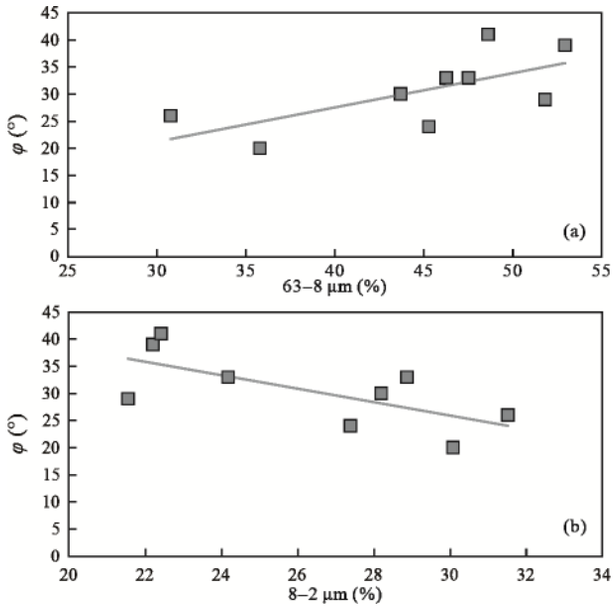

Figure 6. Binary plots displaying the positive and negative trends between friction angle (φ) and 63–8 μm (a) and 8–2 μm (b) granulometrical fractions of widespread landslide samples.

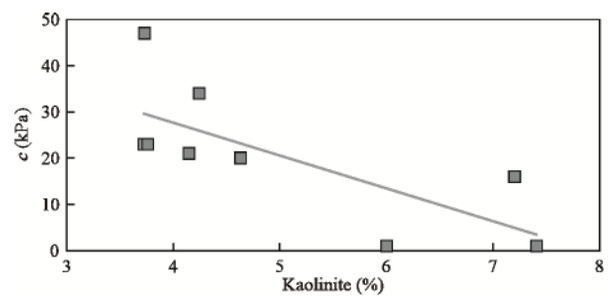

Figure 7. Coesion (c) vs. kaolinite contents in the Montescaglioso widespread sediments.

suggests that a possible weakness zone inside the stratigraphic sequence studied could be present, although further geotechnical data of the S3 core samples are needed to confirm it. However, the above hypothesis seems to be supported by the index properties of the core sediments occurring in the -15 to -20 m range. At this depth, in fact, high values of liquid and plastic limits were detected and the corresponding sediments were classified as very plastic. This is also confirmed by the distribution of S3 core samples in the Casagrande plasticity chart (Casagrande, 1948). In Fig. 8a it is possible to note that all core samples are distributed in the "medium to high plasticity inorganic clay" field and, in particular, sediments from the -15– -20 m level fall in the upper portion of the "high plasticity, inorganic clays" field.

Plasticity is a very important physical property of the fine sediment accounting for its ability to deform at constant volume without cracking or crumbling. It is directly associated with the clay minerals or organic matter content because, depending on the water content, they are able or not to slide relative to each other, with the cohesion between them being maintained. Any decrease/increase in water content results in a decrease/increase of the cation layer thickness and an increase/decrease of the net attractive forces between mineral particles inducing a different rheological behavior of sediments.

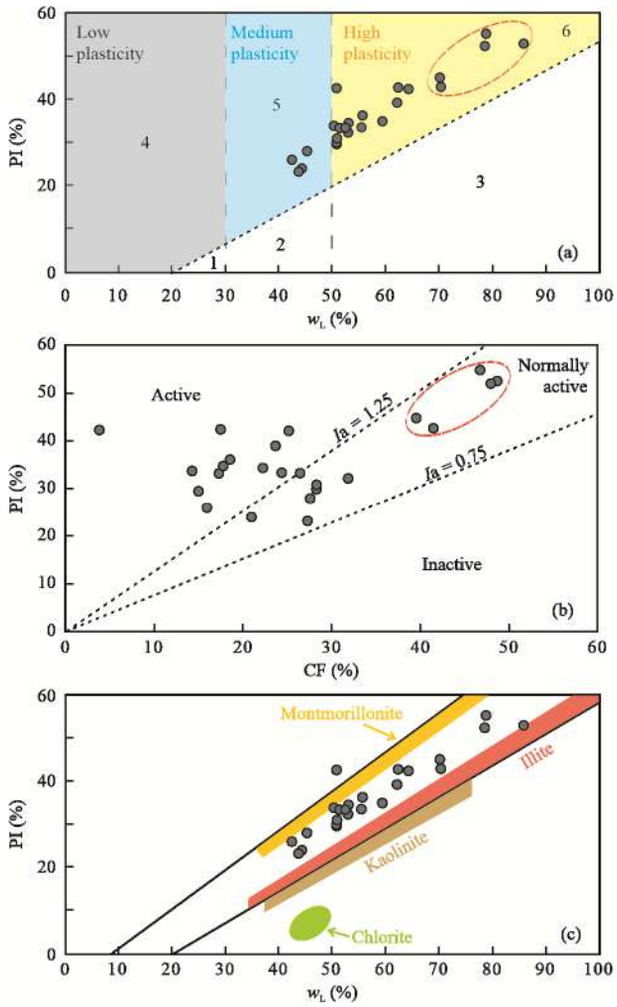

Figure 8. (a) Casagrande Chart and related classification of the investigated core sediments. 1. Low compressibility, inorganic silt; 2. medium compressibility, inorganic and organic silt; 3. high compressibility, inorganic silt and organic clay; 4. low plasticity, inorganic clay; 5. medium plasticity, inorganic clay; 6. high plasticity, inorganic clay. (b) Diagram showing the classification of fine sediments by activity index, *I*a (Facciorusso et al., 2011). (c) Modified plasticity chart displaying the relationships between rheological characters and clay mineralogy. PI. Plasticity index; w_L. liquid limit; CF. clay fraction. Red circles group core samples from the -15 to -20 m level. See the text for further details.

Generally, in fine (predominantly clayey) sediments the PI, which is indicative of the water content range for which sediments assume a plastic behaviour, increases linearly as a function of the percentage of clay fraction (CF), with a different line gradient (i.e., the *I*a = PI/CF) depending on the type of clay minerals present (Cestelli Guidi, 1987). As for the S3 core sediments here analysed (Fig. 8b), a non-linear relation characterizes the samples that, therefore, fall in different portions of the activity index graph proposed by Facciorusso et al. (2011). Furthermore, sediments from the -15 to -20 m stratigraphic level (red circle in Fig. 8b) are distributed far from the other S3 core samples, highlighting their different rheological property.

As suggested by several authors (Ohlmacher, 2000; Holtz

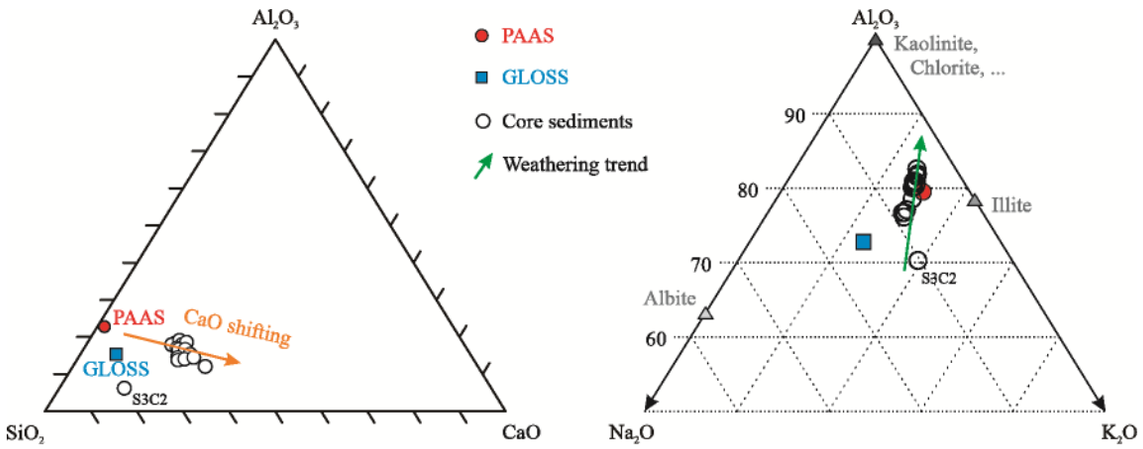

Figure 9. (a) The Al_2O_3-SiO_2-CaO triangular plot shows the shifting of studied sediment composition (white circles) toward the CaO apex, suggesting a relative enrichment of this component to the standard composition of shales (PAAS) or upper-continental-crust sediments (GLOSS). (b) The Al_2O_3-Na_2O-K_2O ternary diagram indicating the weathering trend of the studied core samples. For reference, average compositions of various mineral types are additionally displayed.

and Kovacs, 1981; Casagrande, 1948), clay mineralogy also may affect the plasticity of the sediment. In Fig. 8c, a modified Casagrande plasticity chart is displayed, where ranges of liquid limit and plasticity index for the principal clay minerals (montmorillonite, illite, kaolinite, and chlorite) are shown. In this diagram all S3 core samples, except for the S3C2 sample, plot in an area between the montmorillonite and illite composition in accordance with the XRD analysis results, suggesting that in the study case the mineralogical composition does not affect the sediment rheology significantly.

Physical-mechanical as much as chemical properties of the sediment may change strongly with the weathering degree as well (Summa et al., 2018). Several geochemical indices, including CIA (chemical index of alteration, Nesbitt and Young, 1982), CIW (chemical index of weathering, Harnois, 1988), PIA (plagioclase index of alteration, Fedo et al., 1995), W (weathering index, Ohta and Arai, 2007), have been used in the literature for evaluating and measuring the weathering conditions which affected a source rock. Most of the reliable weathering proxy are based on the assumption that, during chemical alteration of the protolith, the leaching of alkalis (Na^+ and K^+) and Ca^{2+}, and the concentration of Al and Si in the residual sediment are the principal processes that cause the degradation of feldspars and the formation of clay minerals. However, prior to using the weathering indices, much attention has to be paid to the presence of carbonates in sediments. The Ca content relative to carbonates, in fact, may alter the weathering proxy values and lead to misleading conclusions. In this study case, high amounts of carbonate minerals (calcite + dolomite) were detected along the whole S3 core resulting in high CaO percentages of all investigated samples. In addition, a strong negative correlation between Al_2O_3 and CaO (r^2 = -0.74) characterizes the core sediments suggesting the CaO contents are not associated to Al-bearing phases but presumably to carbonates only. Accordingly, the Al_2O_3-SiO_2-CaO ternary plot (Fig. 9a) shows that the Montescaglioso core sediments fall far to the composition of average continental shales (PAAS, Post Archean Australian Shales; Taylor and McLennan, 1985) and upper-continental-crust standard (GLOSS, Global Subducting Sediment; Plank and Langmuir, 1998) because of their higher CaO contents. This obviously makes the use of any aforementioned weathering indices inappropriate for this study case.

However, excluding the CaO, some considerations on weathering degree of sediments may be retrieved by plotting data into the Al_2O_3-Na_2O-K_2O ternary diagram. Since sodium and potassium are mobilised during chemical weathering, changes in their element/Al ratios record a weathering trend. Consequently, the S3 core samples plotted in the triangular diagram of Fig. 9b shows a trend of weathering that varies from bottom to top of the core, indicating a stronger alteration in the upper portion of the deposit.

Such a hypothesis is also supported by the presence of salbands in the upper part of the S3 core only, and by the downward decreasing of I/S amounts. Salbands are considered as the macroscopic evidence of fluid circulation in fine sediments along cracks or fractures (Brondi et al., 1993) where elements mobilization, minerals transformation, oxides and salts precipitation generally occur. In the studied sediments, evidences of a preferential fluid circulation were detected at the macro-scale as much as at the micro-scale. Optical microscope observations of the samples in thin section, in fact, have confirmed the presence of a dense network of veins mostly filled by iron oxi/hydroxides and post-diagenetic calcite, chiefly correlated to secondary processes of solubilisation and/or reprecipitation.

Similarly, the presence of interlayered clay minerals in a sediment may be indicative of chemical alteration processes which affected the primary minerals during weathering (Cuadros et al., 2010; Ferrell et al., 2010). In particular, the variation along the studied profile of the interlayered clays amount suggests that different conditions of weathering occurred along the deposit from top to bottom, with a stronger alteration, maybe due to a more intense fluid circulation, in the upper portion of the deposit.

5 SUMMARY AND CONCLUSIONS

In this paper, the compositional features of the Plio-Pleistocene sediments involved in the studied Montescaglioso Landslide (Basilicata Region, southern Italy) have been investigated with the principal aim to broaden our knowledges on lithological characters of sediments composing the landslide body,

and try to detect possible correlations between lithology and some index properties of fine sediments. Among the several geo-lithological properties considered, only some granulometrical and mineralogical features of the investigated core samples show significant correlations with the rheological indices (Atterberg's limits and plasticity index). In addition, considering the geotechnical data available in literature concerning the widespread landslide sediments here analysed, our results suggest the presence of a possible weakness zone along the studied deposit, represented by the litostratigraphic level having the highest percentage of phyllosilicates and clay fraction. Moreover, a relationship between the clay fraction (CF) contents and the values of w_L and w_P has been detected, suggesting a CF ≈ 38% as possible threshold value for changing the index properties of fine sediments.

Although further detailed studies on fabric of fine sediments in landslide mass and on the correlations between composition and physical-mechanical properties of core sediments are needed, we believe that a multidisciplinary approach may significantly contribute to the identification of weakness and slip zones of landslide terrains mostly in areas, as the Montescaglioso one, where to date doubts rest despite the active monitoring network of the landslide body.

ACKNOWLEDGMENTS

The authors wish to thank the Dipartimento Infrastrutture e Mobilità of the Regione Basilicata – Ufficio Protezione Civile that has financially supported this study and contributed to the coordination and organization of the research activities. A warm thank to Dr. S. Margiotta for his great help during laboratory activities at the IMAA. Finally, many thanks to the editors and reviewers whose comments and suggestions help us to improve the final version of the manuscript. The final publication is available at Springer via https://doi.org/10.1007/s12583-021-1579-8.

REFERENCES CITED

Amanti, M., Chiessi, V., Guarino, P. M., et al., 2016. Back-Analysis of a Large Earth-Slide in Stiff Clays Induced by Intense Rainfalls. In: Aversa, S., Cascini, L., Picarelli, L., et al., eds., Landslides and Engineered Slopes. Experience, Theory and Practice. Proceedings of the 12th International Symposium on Landslides. June 12 – 19, 2016, Napoli, Italy. 317–324. https://doi.org/10.1201/9781315375007

ASTM, 2007. ASTM Book of Standards, PA. ASTM, Philadelphia

Blott, S. J., Pye, K., 2012. Particle Size Scales and Classification of Sediment Types Based on Particle Size Distributions: Review and Recommended Procedures. *Sedimentology*, 59(7): 2071 – 2096. https://doi.org/10.1111/j.1365-3091.2012.01335.x

Bonomo, A. E., 2015. Composition and Properties of Sediments Involved in the Montescaglioso Landslide (Basilicata, Southern Italy): [Dissertation]. Geoenvironmental Resources and Risks, School of Science and Technology, Geology division, University of Camerino, Camerino

Bozzano, F., Caporossi, P., Esposito, C., et al., 2017. Mechanism of the Montescaglioso Landslide (Southern Italy) Inferred by Geological Survey and Remote Sensing. Abstract in 4th World Landslide Forum. May 29 – June 2, 2017, Ljubljana, Slovenia. 97 – 106. https://doi. org/10.1007/978-3-319-53498-5_12

Brondi, A., Colica, A., Conti, P., et al., 1993. Joints in Clays of the Neogenic Basin of Siena. *Mineralogica et Petrographica Acta*, 35: 51–65

Caporossi, P., Mazzanti, P., Bozzano, F., 2018. Digital Image Correlation (DIC) Analysis of the 3 December 2013 Montescaglioso Landslide (Basilicata, Southern Italy): Results from a Multi-Dataset Investigation. *ISPRS International Journal of Geo-Information*, 7(9): 372. https://doi.org/10.3390/ijgi7090372

Carlà, T., Raspini, F., Intrieri, E., et al., 2016. A Simple Method to Help Determine Landslide Susceptibility from Spaceborne InSAR Data: The Montescaglioso Case Study. *Environmental Earth Sciences*, 75(24): 1–12. https://doi.org/10.1007/s12665-016-6308-8

Casagrande, A., 1948. Classification and Identification of Soils. *Transactions of the American Society of Civil Engineers*, 113(1): 901–930. https://doi.org/10.1061/taceat.0006109

Cavalcante, F., Fiore, S., Lettino, A., et al., 2007. Illite-Smectite Mixed Layers in Sicilide Shales and Piggy-Back Deposits of the Gorgoglione Formation (Southern Appennines): Geological Inferences. *Bollettino della Societa Geologica Italiana*, 126: 241–254

Cestelli Guidi, C., 1987. Geotecnica e Tecnica delle Fondazioni (Geotechnical and Fundation Engineering). Hoepli, U., Milano. XXXII-864 (in Italian)

Cuadros, J., Fiore, S., Huertas, F. J., 2010. Introduction to Mixed-Layer Clay Minerals. In: Fiore, S., Cuadros, J., Huertas, F. J., eds., Interstratified Clay Minerals: Origin, Characterization and Geochemical Significance. AIPEA Educational Series, Pub. No. 1, Digilabs, Bari, Italy. 175

Dai, F. C., Lee, C. F., Ngai, Y. Y., 2002. Landslide Risk Assessment and Management: An Overview. *Engineering Geology*, 64(1): 65–87. https://doi.org/10.1016/s0013-7952(01)00093-x

D'Ecclesiis, G., Lorenzo, P., 2006. Relict Landslides in the Deposits of Adriatic Foredeep: The Landslide of Madonna della Nuova (Montescaglioso, Basilicata). *Giornale di Geologia Applicata*, 4: 257–262 (in Italian with English Abstract)

Facciorusso, J., Madiai, C., Vannucchi, G., 2011. Dispense di Geotecnica (Lecture Notes of Geotechnics). Pisa University Press, Pisa (in Italian)

Fedo, C. M., Wayne Nesbitt, H., Young, G. M., 1995. Unraveling the Effects of Potassium Metasomatism in Sedimentary Rocks and Paleosols, with Implications for Paleoweathering Conditions and Provenance. *Geology*, 23(10): 921 – 924 https://doi. org/10.1130/0091-7613(1995)0230921:uteopm>2.3.co;2

Ferrell, R. E. Jr., Aparicio, P., Forsman, J., 2010. Interstratified Clay Minerals in the Weathering Environment. In: Fiore, S., Cuadros, J., Huertas, F. J., eds., Interstratified Clay Minerals: Origin, Characterization and Geochemical Significance. AIPEA Educational Series, Pub. No. 1, Digilabs, Bari, Italy. 175

Franzini, M., Leoni, L., Saitta, M., 1972. A Simple Method to Evaluate the Matrix Effects in X-Ray Fluorescence Analysis. *X-Ray Spectrometry*, 1(4): 151–154. https://doi.org/10.1002/xrs.1300010406

Franzini, M., Leoni, L., Saitta, M., 1975. Revisione di una Metodologia Analitica per Fluorescenza X Basata sulla Correzione Completa degli Effetti di Matrice (Review of an Analytical Methodology for X-Ray Fluorescence Based on the Complete Correction of Matrix Effects). *Società Italiana di Mineralogia e Petrologia*, 31: 365–378 (in Italian)

Gariano, S. L., Guzzetti, F., 2016. Landslides in a Changing Climate. *Earth-Science Reviews*, 162: 227 – 252. https://doi. org/10.1016/j. earscirev. 2016.08.011

Giannecchini, R., Galanti, Y., D'Amato Avanzi, G., et al., 2016. Probabilistic Rainfall Thresholds for Triggering Debris Flows in a Human-Modified Landscape. *Geomorphology*, 257: 94–107. https://doi.org/10.1016/j.geomorph.2015.12.012

Guzzetti, F., Cardinali, M., Reichenbach, P., 1994. The AVI Project: A Bibliographical and Archive Inventory of Landslides and Floods in Italy. *Environmental Management*, 18(4): 623 – 633. https://doi. org/10.1007/bf02400865

Guzzetti, F., Tonelli, G., 2004. Information System on Hydrological and Geomorphological Catastrophes in Italy (SICI): A Tool for Managing Landslide and Flood Hazards. *Natural Hazards and Earth System Sciences*, 4(2): 213–232. https://doi.org/10.5194/nhess-4-213-2004

Harnois, L., 1988. The CIW Index: A New Chemical Index of Weathering. *Sedimentary Geology*, 55(3/4): 319–322. https://doi.org/10.1016/0037-0738(88)90137-6

Holtz, R. D., Kovacs, W. D., 1981. An Introduction to Geotechnical Engineering. Prentice-Hall, Englewood Cliffs, New Jersey, USA

Igwe, O., Mode, W., Nnebedum, O., et al., 2014. The Analysis of Rainfall-Induced Slope Failures at Iva Valley Area of Enugu State, Nigeria. *Environmental Earth Sciences*, 71(5): 2465 – 2480. https://doi. org/10.1007/s12665-013-2647-x

Igwe, O., 2015. The Geotechnical Characteristics of Landslides on the Sedimentary and Metamorphic Terrains of South-East Nigeria, West Africa. *Geoenvironmental Disasters*, 2: 1. https://doi. org/10.1186/s40677-014-0008-z

Kenney, T. C., 1967. The Influence of Mineralogical Composition on the Residual Shear Strength of Natural Soils. In: Proc. Geotech. Conf. on Shear Strength Properties of Natural Soils and Rocks, Oslo. 123–129

Kenney, T. C., 1977. Residual Shear Strength of Mineral Mixtures. 9th International Conference on Soil Mechanics and Foundation Engineering, Tokyo. 155–160

Manconi, A., Casu, F., Ardizzone, F., et al., 2014. Brief Communication: Rapid Mapping of Landslide Events: The 3 December 2013 Montescaglioso Landslide, Italy. *Natural Hazards and Earth System Sciences*, 14(7): 1835 – 1841. https://doi. org/10.5194/nhess-14-1835-2014

Mesri, G., Cepeda-Diaz, A. F., 1986. Residual Shear Strength of Clays and Shales. *Géotechnique*, 36(2): 269 – 274. https://doi. org/10.1680/geot.1986.36.2.269

Napolitano, E., Fusco, F., Baum, R. L., et al., 2016. Effect of Antecedent-Hydrological Conditions on Rainfall Triggering of Debris Flows in Ash-Fall Pyroclastic Mantled Slopes of Campania (Southern Italy). *Landslides*, 13(5): 967 – 983. https://doi. org/10.1007/s10346-015-0647-5

Nesbitt, H. W., Young, G. M., 1982. Early Proterozoic Climates and Plate Motions Inferred from Major Element Chemistry of Lutites. *Nature*, 299(5885): 715–717. https://doi.org/10.1038/299715a0

Ohlmacher, G. C., 2000. The Relationship between Geology and Landslide Hazards of Atchison, Kansas, and Vicinity. *Current Research in Earth Sciences*, 244: 1–16. https://doi.org/10.17161/cres.v0i244.11833

Ohta, T., Arai, H., 2007. Statistical Empirical Index of Chemical Weathering in Igneous Rocks: A New Tool for Evaluating the Degree of Weathering. *Chemical Geology*, 240(3/4): 280–297. https://doi.org/10.1016/j.chemgeo.2007.02.017

Pellicani, R., Spilotro, G., Ermini, R., et al., 2016. The Large Montescaglioso Landslide of December 2013 After Prolonged and Severe Seasonal Climate Conditions. Abstract in 12th International Symposium on Landslides, June 12–19, Naples, Italy. 1591–1597

Pellicani, R., Argentiero, I., Manzari, P., et al., 2019. UAV and Airborne LiDAR Data for Interpreting Kinematic Evolution of Landslide Movements: The Case Study of the Montescaglioso Landslide (Southern Italy). *Geosciences*, 9(6): 248. https://doi.org/10.3390/geosciences9060248

Perrone, A., Piscitelli, S., Gueguen, E., et al., 2014. Electrical Resistivity Tomographies for the Geophysical Characterization of the Montescaglioso Slope (MT) Affected by the 3 December 2013 Landslide). [2021-8-20]. http://www. emergenza. regione. basilicata. it/emerg_alluv_2011/files/docs/10/05/16/DOCUMENT_FILE_100516.pdf (in Italian)

Plank, T., Langmuir, C. H., 1998. The Chemical Composition of Subducting Sediment and Its Consequences for the Crust and Mantle. *Chemical Geology*, 145(3/4): 325 – 394. https://doi. org/10.1016/s0009-2541(97)00150-2

Raspini, F., Ciampalini, A., del Conte, S., et al., 2015. Exploitation of Amplitude and Phase of Satellite SAR Images for Landslide Mapping: The Case of Montescaglioso (South Italy). *Remote Sensing*, 7(11): 14576–14596. https://doi.org/10.3390/rs71114576

Rosi, A., Segoni, S., Catani, F., et al., 2012. Statistical and Environmental Analyses for the Definition of a Regional Rainfall Threshold System for Landslide Triggering in Tuscany (Italy). *Journal of Geographical Sciences*, 22(4): 617–629. https://doi.org/10.1007/s11442-012-0951-0

Schultz, L. G., 1964. Quantitative Interpretation of Mineralogical Composition from X-Ray and Chemical Data for the Pierre Shale. Professional Paper 391-C: 1–31. https://doi.org/10.3133/pp391c

Shaw, D. B., Stevenson, R. G., Weaver, C. E., et al., 1971. Interpretation of X-Ray Diffraction Data. In: Carver, R. E., ed., Procedures in Sedimentary Petrology. Wiley, New York. 554–557

Skempton, A. W., 1964. Long-Term Stability of Clay Slopes. *Géotechnique*, 14(2): 77–102. https://doi.org/10.1680/geot.1964.14.2.77

Summa, V., 2000. Analisi Granulometrica dei Sedimenti. In: Metodi di Analisi di Materiali Argillosi. V Corso di Formazione AIPEA, Association Internationalle Pour l'Etude des Argiles, Gruppo Italiano. 19–29

Summa, V., Tateo, F., Medici, L., et al., 2007. The Role of Mineralogy, Geochemistry and Grain Size in Badland Development in Pisticci (Basilicata, Southern Italy). *Earth Surface Processes and Landforms*, 32(7): 980–997. https://doi.org/10.1002/esp.1449

Summa, V., Tateo, F., Giannossi, M. L., et al., 2010. Influence of Clay Mineralogy on the Stability of a Landslide in Plio-Pleistocene Clay Sediments near Grassano (Southern Italy). *CATENA*, 80(2): 75 – 85. https://doi.org/10.1016/j.catena.2009.09.002

Summa, V., Margiotta, S., Colaiacovo, R., et al., 2015. The Influence of the Grain-Size, Mineralogical and Geochemical Composition on the Verdesca Landslide. *Natural Hazards and Earth System Sciences*, 15(1): 135–146. https://doi.org/10.5194/nhess-15-135-2015

Summa, V., Margiotta, S., Medici, L., et al., 2018. Compositional Characterization of Fine Sediments and Circulating Waters of Landslides in the Southern Apennines-Italy. *CATENA*, 171: 199 – 211. https://doi.org/10.1016/j.catena.2018.07.009

Taylor, S. R., McLennan, S. M., 1985. The Continental Crust: Its Composition and Evolution. *The Journal of Geology*, 94(4): 57–72

Tropeano, M., Sabato, L., Pieri, P., 2002. Filling and Cannibalization of a Foredeep: The Bradanic Trough, Southern Italy. *Geological Society, London, Special Publications*, 191(1): 55 – 79. https://doi.org/10.1144/gsl.sp.2002.191.01.05

Whitney, D. L., Evans, B. W., 2010. Abbreviations for Names of Rock-Forming Minerals. *American Mineralogist*, 95(1): 185–187. https://doi.org/10.2138/am.2010.3371

Yalcin, A., 2007. The Effects of Clay on Landslides: A Case Study. *Applied Clay Science*, 38(1/2): 77–85. https://doi.org/10.1016/j.clay.2007.01.007